Kinetics of the Heterogeneous Reaction $HNO_3(g) + NaBr(s) \leftrightarrow HBr(g) + NaNO_3(s)$

Ming-Taun Leu,* Raimo S. Timonen, and Leon F. Keyser

Earth and Space Sciences Division, Jet Propulsion Laboratory, California Institute of Technology, Pasadena, California 91109

Received: August 22, 1996; In Final Form: October 22, 1996[⊗]

The kinetics of the heterogeneous reaction $HNO_3(g) + NaBr(s) \leftrightarrow HBr(g) + NaNO_3(s)$ has been investigated at 296 K using a fast-flow reactor coupled to an electron-impact ionization mass spectrometer. The concentrations of HNO_3 and HBr in the presence of salts were monitored mass spectrometrically, and their decay rates were used to obtain uptake coefficients. The sizes of NaBr and $NaNO_3$ granules were measured using an optical microscope, and their specific surface areas were estimated by a well-known relationship, $Sg = 6/d\rho_t$, where d is the average diameter of the granule and ρ_t is the true density of the NaBr or $NaNO_3$ substrate. Our observations indicate that the uptake process comprises both physical adsorption and chemical reaction. The uptake coefficients for the forward and reverse processes, after accounting for internal surfaces by means of a mathematical model of surface reaction and pore diffusion, were found to be $(2.8 \pm 0.5) \times 10^{-3}$ and $(1.2 \pm 0.2) \times 10^{-2}$ at 296 K, respectively. The error limits represent one standard deviation precision only. The implications for atmospheric chemistry in the marine boundary layer and Arctic troposphere are discussed.

Introduction

The forward reaction (1f) between gaseous HNO_3 and solid NaBr is of interest for the following reasons. First, heterogeneous reactions involving NaBr have been suggested to play an important role in ozone depletion in the Arctic troposphere.[1−3] Recent field studies in the spring at Alert, Canada, show that ground-level ozone concentrations decrease dramatically in a period of time ranging from a few hours to a few days.[4−6] The studies also demonstrate that there is a strong correlation between ozone destruction and filterable bromine (the sum of Br on particles and gaseous species, such as HBr efficiently collected by a combination Teflon/nylon filter). Also, both gaseous and particulate bromine compounds have been found in the marine boundary layer around the world.[7−9] Thus, bromine photochemistry, including some heterogeneous reactions, has been invoked to explain the ozone loss. Second, numerous studies of heterogeneous NaCl reactions have been documented in the literature.[10−13] These were motivated by the discovery of salt particles in the stratosphere after the El Chichon volcanic eruptions[14] and the subsequent measurement of the enhancement of hydrochloric acid.[15−17] Third, reactions on NaCl aerosols in the marine boundary layer have been used to explain measurements of HCl and HNO_3.[18−20] A study of bromine heterogeneous reactions is a useful extension of this work.

$$HNO_3\,(g) + NaBr\,(s) \leftrightarrow HBr\,(g) + NaNO_3\,(s) \qquad \Delta H°(298\text{K}) = -1.9\ \text{kcal/mol} \quad (1)$$

In a previous study of reaction 1f, Fenter et al.[12] used a low-pressure Knudsen cell and obtained a value of $\gamma(1f) = 0.028$ at room temperature. This value was based on only one experiment and was comparable to the reaction probabilities on other salts. Moreover, the result was not corrected for the effect of internal surface area of the NaBr substrate. To our knowledge, there is no previous study of the reverse reaction 1r.

In this article we report experimental results for both reactions 1f and 1r. By using a fast-flow reactor coupled to a differentially-pumped quadrupole mass spectrometer, the kinetic mechanism was investigated. Moreover, a mathematical model of surface reaction and pore diffusion was used to obtain uptake coefficients in a manner similar to our previous studies on reactions of NaCl with $ClONO_2$, HNO_3, and N_2O_5.[10,11] The implication for atmospheric chemistry in the marine boundary layer and Arctic troposphere will be briefly discussed.

Experimental Method

The uptake coefficient measurement was performed in a fast-flow reactor coupled to an electron-impact ionization mass spectrometer, as shown in Figure 1.[10,11,21] The flow reactor was made of borosilicate glass, and its dimensions were 20.0 cm length and 1.8 cm inside diameter. The bottom of the reactor was recessed and flattened in order to hold the NaBr or $NaNO_3$ substrates in place. The depth of the recess was about 0.33 cm. Temperature was regulated by circulating cold methanol through a jacket surrounding the flow reactor, and the temperature was measured by a thermocouple attached to the middle section. The pressure inside the reactor was monitored by a high-precision capacitance manometer which was located about 7 cm from the reactor at the downstream end. The measured pressure was corrected for the viscous pressure gradient between the measurement point and the midpoint of the reactor. The carrier gas, helium, was admitted to the reactor through a side-arm inlet. The gas-phase reactants, HNO_3 or HBr, were added through a sliding borosilicate injector. The average flow velocity in the flow-tube reactor was calculated to be between 1400 and 1800 cm/s. A large metal valve located at the downstream end of the reactor was used to regulate the flow velocity.

HNO_3 was prepared by reacting H_2SO_4 (96 wt %) with reagent grade $NaNO_3$ (99%) in vacuum, and the nitric acid vapor was collected in a Pyrex vessel at liquid nitrogen temperature. The HNO_3 thus prepared was further purified by vacuum distillation at 195 K. HBr was mixed with

* Author to whom correspondence should be addressed.
⊗ Abstract published in *Advance ACS Abstracts,* January 1, 1997.

S1089-5639(96)02606-0 CCC: $14.00

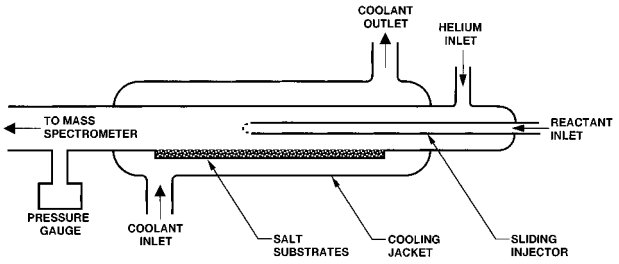

Figure 1. Schematic diagram of a neutral fast-flow reactor coupled to an electron-impact ionization mass spectrometer. The bottom of the reactor was recessed and flattened for the preparation of salt substrates. See text for details.

helium in a 5 L glass vessel, and its flow rate was measured by a mass flowmeter. HNO_3 and HBr were monitored by the mass spectrometer using $m/e = 46$ and 80 amu, respectively.

Two batches of NaBr were obtained from E. Merck Corp. The size and shape of the granules were examined by using an optical microscope. The typical shape was cubic, and the average sizes were found to be about 0.272 ± 0.081 (1σ, assuming a normal distribution) mm for batch 1 and 0.249 ± 0.100 (1σ) mm for batch 2, respectively. The specific surface area, Sg, can be calculated from the average crystal size by using[22]

$$\mathrm{Sg} = 6/\rho_t d \tag{2}$$

where ρ_t is the true density of NaBr (3.204 g/cm^3)[23] and d is the granule size. One batch of $NaNO_3$ was purchased from Fisher, and its average size was about $0.190 \pm 0.091(1\sigma)$ mm. Another batch was supplied by J. T. Baker, and the average size was slightly smaller, 0.145 ± 0.107 (1σ) mm. The true density of $NaNO_3$ is 2.261 g/cm^3.[23] In typical experiments these substrates were placed in the reactor and then were baked under vacuum for at least 4 h. However, in some experiments they were not heated in order to test the effect of surface moisture on the reactivity. The results will be discussed later.

The procedure used in determining the reaction probability is similar to that in our previous studies[10,11] and will be briefly discussed as follows. The loss rates of HNO_3 and HBr were measured as a function of inlet position, z. The reaction time was calculated by using $t = z/v$, where v is the average flow velocity. In each experiment we calculated the cross-sectional area of the reactor and then the flow velocity. The first-order rate constant, k_s, was calculated from the slope of a linear least-squares fit to the experimental data. The axial gas-phase diffusion correction to k_s was made by using the following equation:[24]

$$k_g = k_s(1 + k_s D/v^2) \tag{3}$$

The diffusion coefficients of HNO_3 and HBr in helium were estimated to be pD = 495 and 440 Torr cm^2 s^{-1} at 296 K, respectively.[25] The rate corrected for gas-phase diffusion is designated as k_g.

For radial gas-phase diffusion, it is more difficult to estimate the correction to k_s because the reactor is no longer a fully symmetric cylindrical tube. If we use the full reactor radius of 0.9 cm in the calculation, the correction is relatively small, less than 10%. Since this correction is not precise, we neglected it in the data analysis.

On the basis of the geometric area (S) which was used to hold the NaBr or $NaNO_3$ substrates and the volume (V) of the reactor, the reaction probability, γ_g, was then calculated by using the following equation:[26]

$$\gamma_g = 4k_g V/\omega S \tag{4}$$

where ω is the average molecular velocity for HNO_3 or HBr at 296 K. Note that this equation is valid for $\gamma_g < 0.1$ only, which holds for the present experiments.

To account for the surfaces of the salt granules beneath the top layer, we used an analysis recently developed and successfully applied to heterogeneous reactions on porous ice films.[27] We model the NaBr or $NaNO_3$ substrates as hexagonal close-packed (HCP) spherical granules stacked in layers. For this model, the following equation holds:

$$\gamma_t = \gamma_g \pi^{-1} 3^{1/2}\{1 + \eta[2(N_L - 1) + (3/2)^{1/2}]\}^{-1} \tag{5}$$

where γ_t is the true reaction probability for reactions 1 and 2 and N_L is the number of granule layers or the ratio of the thickness of the salt substrates to the average granule size. In eq 5, η is the effectiveness factor, which is the fraction of the NaBr or $NaNO_3$ surface that participates in the reaction. This factor is determined by the relative rates of pore diffusion to surface reaction and is given by

$$\eta = \phi^{-1} \tanh \phi \tag{6}$$

$$\phi = (h_i/d)[3\rho_b/2(\rho_t - \rho_b)](3\tau\gamma_t)^{1/2} \tag{7}$$

where h_i is the internal thickness of the salt substrates, d is the average size of granules, ρ_b is the bulk density, ρ_t is the true density, and τ is a tortuosity factor. Typically, this factor is between 1.7 and 4.[28] In our data analysis, we used a value of 2. This type of calculation has been successfully used in previous publications.[10,11]

In general, the magnitude of the corrections that convert γ_g to γ_t is less than a factor of 3 for $\gamma_t > 0.1$. However, for $\gamma_t < 0.1$, the corrections become much larger.[26,27] The possible uncertainties in the correction factors can be estimated by assessing the expected errors introduced by uncertainties in N_L, τ, and the type of packing (bulk density). For an uncertainty in N_L of ± 2 within the range used, the errors in the correction factors are less than 15%. For $\tau = 2$ or 3,[28] the error in the correction factors is less than $\pm$20%. For layer packing between simple cubic packing (SCP) and HCP, the correction factor error ranges over $\pm$25%. Including the errors ($\sim$15$-$25%) associated with the measurements of temperature, total pressure, flow rates, and external gas-phase diffusion correction, we estimate that the systematic error is about a factor of 2.

Results and Discussion

$HNO_3 + NaBr \rightarrow HBr + NaNO_3$ (1f). The uptake of HNO_3 in the presence of NaBr is shown in Figure 2. The experimental conditions were $p(HNO_3) = 6.7 \times 10^{-7}$ Torr, m(NaBr) = 28 g, $p = 0.462$ Torr, and $v = 1716$ cm/s. Initially the sliding injector was positioned downstream of the NaBr substrate. After about 4 min, the reaction was started by moving the injector upstream from the substrate. The uptake or loss of HNO_3 coincided with the appearance of HBr from the NaBr surface. The gradual rise in the HNO_3 signal was an indication of surface deactivation. At about 30 min, the injector was moved downstream and the HBr signal dropped to near zero, while the HNO_3 signal was higher than the initial value. This sequence was repeated one more time at about 36 and 60 min. After calibration of HNO_3 and HBr signals, the uptake of HNO_3 was found to be about 1.8×10^{17} molecules and the yield of HBr was found to be about 6.1×10^{16} molecules. These

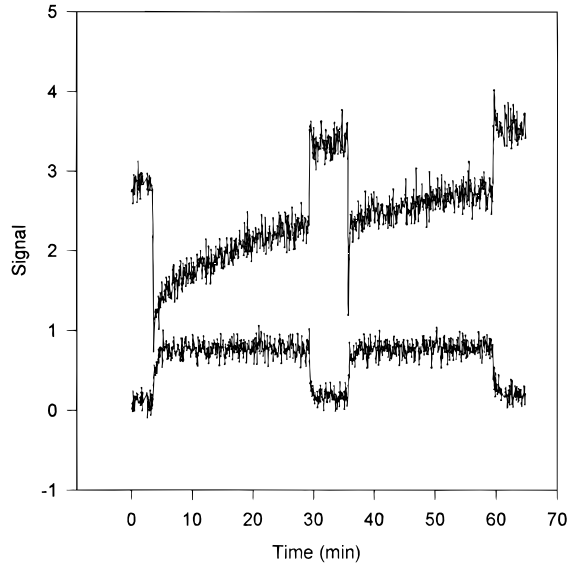

Figure 2. Uptake of HNO_3 by NaBr (HNO_3(g) + NaBr(s) → HBr(g) + $NaNO_3$(s)) at 296 K. Both the HNO_3 loss (upper curve) and HBr growth (lower curve) were monitored.

observations suggest that the yield of HBr is about 34% of the uptake of HNO_3. Furthermore, the observation of an increase in the HNO_3 signal when the injector was moved downstream is evidence that some of the HNO_3 may also be physically adsorbed on the NaBr surface. In a separate experiment, we measured the physical uptake of HNO_3 on the $NaNO_3$ substrates and we did not find any reaction products formed. Similarly, some of the HBr may also stay on the surface of salts. This finding is consistent with the observation of the uptake of HCl on NaCl powders reported by Fenter et al.[12] Thus, the uptake of HNO_3 on the surface of NaBr comprises two components: physical uptake and reactive uptake.

The uptake coefficients of HNO_3 on NaBr were measured by monitoring HNO_3 signals while moving the injector from downstream to upstream and by calculating the decay rate of HNO_3. The procedure has been discussed in the preceding section. Under plug-flow conditions, the decay of HNO_3 is given by the equation

$$\ln[S(z)] = -k_s(z/v) + \ln[S(0)] \qquad (8)$$

Typical data for the HNO_3 loss as a function of injector position are shown in Figure 3. The experimental conditions were $p(HNO_3) = 7.0 \times 10^{-7}$ Torr, m(NaBr) = 28 g, $v = 1611$ cm/s, and $p = 0.372$ Torr. The salt was baked for a few hours at a temperature of 443 K. We repeated the same procedure several times and obtained a value of $\gamma_g(1f) = 0.022$ in this experiment. The total exposure time was always less than 10−20 s in order to prevent any significant surface deactivation. After correcting for the internal surface area, we found $\gamma_t(1f) = 0.0019$. Moreover, we have used two batches of samples supplied from Merck (see Experimental Method) and performed the experiments by using the dry salts or unbaked samples in order to check the effect of moisture on the uptake. The results are summarized in Table 1. The data obtained by using the unbaked salts appear to be about 20% greater than those for baked salts. But, the difference is within the quoted uncertainties and is considered to be insignificant. The average value of these measurements is $\gamma_t(1f) = (2.8 \pm 0.5) \times 10^{-3}$ at 296 K. The error limit represents one standard deviation. It is also noted that on the basis of the external geometric area of the NaBr substrate, $\gamma_g(1f) = 0.027$, about a factor of 10 greater than γ_t-(1f) due to the effect of the internal surface area.

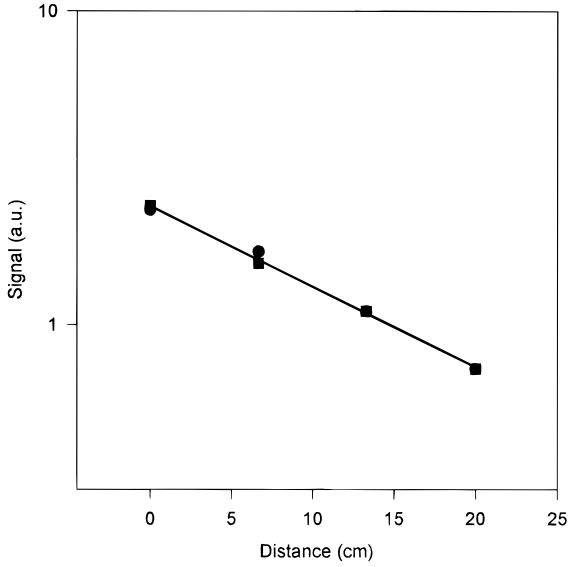

Figure 3. Loss of HNO_3 signals as a function of injector position at 296 K (HNO_3(g) + NaBr(s)). Closed squares are for data obtained when the injector was moved from downstream to upstream. Closed circles are for data obtained when the injector was moved from upstream to downstream.

TABLE 1: Summary of the Reaction Probability Measurements for the Reaction HNO_3(g) + NaBr(s) → HBr(g) + $NaNO_3$(s) at 296 K[a]

NaBr substrate	no. of expts	γ_g ($\times 10^{-2}$)	γ_t ($\times 10^{-3}$)
baked (Merck 1)	51	2.5 ± 0.3	2.5 ± 0.6
baked (Merck 2)	12	2.6 ± 0.4	2.6 ± 0.7
unbaked (Merck 1)	42	2.8 ± 0.4	3.0 ± 0.7
unbaked (Merck 2)	8	2.9 ± 0.1	3.1 ± 0.2
		av: 2.7 ± 0.4	av: 2.8 ± 0.5

[a] The errors indicate one standard deviation.

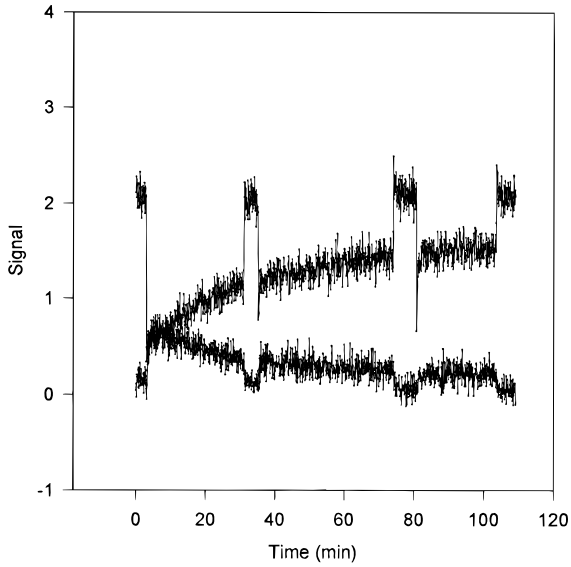

Figure 4. Uptake of HBr by $NaNO_3$ (HBr(g) + $NaNO_3$(s) → HNO_3-(g) + NaBr(s)) at 296 K. Both the HBr loss (upper curve) and HNO_3 growth (lower curve) were monitored.

HBr + $NaNO_3$ → HNO_3 + NaBr (1r). We also studied the uptake of HBr in the presence of $NaNO_3$ (1r) by using a procedure similar to that used for reaction 1f. One example of the experiment is shown in Figure 4. The uptake of HBr and the yield of HNO_3 decreased during exposure to $NaNO_3$, suggesting that some deactivation of the surface may have occurred. The yield of HNO_3 was only about 10−30% of the

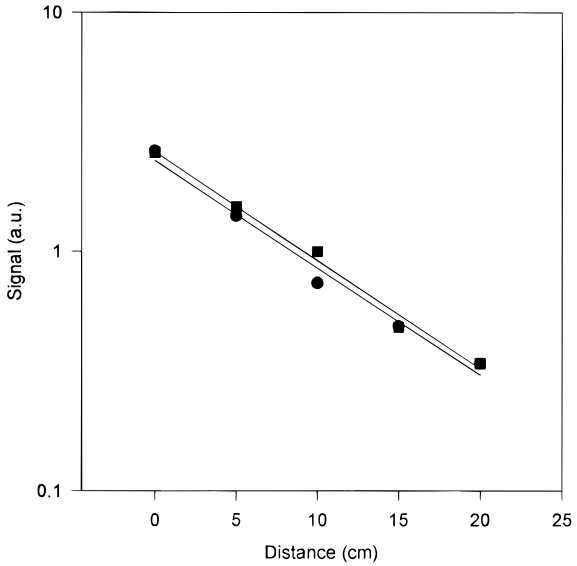

Figure 5. Loss of HBr signals as a function of injector position at 296 K ($HBr(g) + NaNO_3(s)$). Closed squares are for data obtained when the injector was moved from downstream to upstream. Closed circles are for data obtained when the injector was moved from upstream to downstream.

TABLE 2: Summary of the Reaction Probability Measurements for the Reaction $HBr(g) + NaNO_3(s) \rightarrow HNO_3(g) + NaBr(s)$ at 296 K[a]

$NaNO_3$ substrate	no. of expts	γ_g ($\times 10^{-2}$)	γ_t ($\times 10^{-2}$)
baked (Fisher)	10	6.5 ± 0.8	1.1 ± 0.2
baked (Baker)	59	6.7 ± 0.9	1.2 ± 0.3
unbaked (Baker)	20	6.6 ± 0.9	1.2 ± 0.2
		av: 6.6 ± 0.9	av: 1.2 ± 0.2

[a] The errors indicate one standard deviation.

HBr uptake. This implies that both physical and reactive uptakes are occurring. Desorption of HBr was not observed during the experiment on the basis of the observation that the HBr signal was nearly constant when the injector was moved downstream (see Figure 4). This implies that HBr is more strongly adsorbed on $NaNO_3$ than HNO_3 is on NaBr (see Figure 2).

The uptake coefficient was also measured by placing about 19 g of $NaNO_3$ inside the flow reactor and by monitoring the decay rate of HBr while moving the injector from downstream to upstream and then moving the injector from upstream to downstream. The data are shown in Figure 5. The experimental conditions were $p(HBr) = 6.5 \times 10^{-7}$ Torr, $v = 1737$ cm/s, and $p = 0.470$ Torr. A value of $\gamma_g(1r) = 0.076$ was determined. We repeated the same procedure for correction of the internal surface area and obtained a consistent value of $\gamma_t(1r) = 0.014$ in this experiment. The correction factor is about a factor of 5. Again, we used two batches of samples, one supplied from Fisher Co. and another from Baker Co. The results are summarized in Table 2. It appears that there is no difference between the data for dry salts and unbaked salts. The average value of these measurements is $\gamma_t(1r) = 0.012 \pm 0.002$ at 296 K. The error limit represents one standard deviation. It appears that the rate for the forward reaction (1f) is about a factor of 4 smaller than that for the reverse reaction (1r).

The change in entropy for reaction 1 can be estimated to be $\Delta S°(298K) = -9.17$ cal mol^{-1} K^{-1} on the basis of the ratio $k(1f)/k(1r)$ measured in this experiment. The result is in good agreement with the value of $\Delta S°(298K) = -9.08$ cal mol^{-1} K^{-1} obtained using thermodynamic data.[23] This suggests that our measurements of uptake coefficients for reaction 1 are reasonable.

In a previous investigation by Fenter et al.[12] using a Knudsen cell reactor, they obtained a value of 0.028 for the uptake of HNO_3 on NaBr on the basis of only one experiment. Surprisingly, they found that the uptake coefficients are identical for a variety of salts, such as NaCl, KBr, $NaNO_3$, KCl, and NaBr. The same result for the nonreactive salt, $NaNO_3$, suggests that the uptake process is physical adsorption instead of chemical reaction. It should be noted that their value is not corrected for the porous nature of the salts. Our result of $\gamma_g = 0.027$ (see Table 1) obtained by using the external geometric area of the salt substrates, is in excellent agreement with their value of 0.028, despite the difference in experimental methods used.

Very recently, Fenter et al.[29] repeated the same experiment using the Knudsen cell technique for the uptake of HNO_3 and N_2O_5 on NaCl and KBr. The results for the N_2O_5 reactions clearly show that the uptake coefficients are strongly mass dependent. They used the theoretical models[26,27] we have previously developed for the surface reaction and pore diffusion in the investigation of heterogeneous reactions on ice and salt. The correction factors range from 5 to 30, depending upon the substrates used in their experiments. Thus, our model holds very well for slow reactions ($\gamma \sim 10^{-3}$). However, the results for the faster HNO_3 reactions (the uptake coefficients are about 1 or 2 orders of magnitude greater than the N_2O_5 reactions) show no mass dependence. They went on to suggest that "sticky" molecules like nitric acid do not diffuse through the top layer and thus internal surface areas may not be available for reactions. However, their results shown in Table 4 of ref 29 are rather scattered (a factor of 4 or 5 for the NaCl reaction and almost a factor of 10 for the KBr reaction) and are inconsistent with their conclusions.

In the flow tube studies,[11] the experiments are carried out at 0.4 Torr in helium and HNO_3 at a partial pressure about 10^{-7} Torr. However, in a Knudsen cell experiment a total pressure of HNO_3 of about 10^{-4} Torr is used.[29] Surface deactivation at higher HNO_3 concentrations on the top layer of salt may occur in the experiments carried out by Fenter et al. In the flow tube studies a small, but noticeable, decrease (about a factor 2) in the uptake coefficients when the partial pressure of HNO_3 was varied from 7.9×10^{-8} to 1.1×10^{-6} Torr (see Table 1 in ref 11). We believe that this effect is due to surface deactivation, thus reducing the observed uptake coefficient. However, Fenter et al. used a HNO_3 pressure ($\sim 10^{-4}$ Torr) significantly greater than that used in flow tube studies. For the larger uptake coefficient, this effect may be serious. We suggest that much lower reactant concentrations should be used. It is further noted that the reactant pressures used in Knudsen cell experiments do not mimic atmospheric conditions in both the troposphere and stratosphere.

The uptake of HNO_3 on NaCl ($\gamma_t = 0.013$) measured previously in our laboratory[11] is about a factor of 5 greater than the uptake of HNO_3 on NaBr reported in this work. The difference may be associated with the energetics (for example, -3.3 kcal/mol for the NaCl reaction and -1.9 kcal/mol for the NaBr reaction) of these reactions. However, it should be noted that our understanding of heterogeneous reactions is rather poor compared with homogeneous gas-phase reactions and we believe that presently there is no sound theoretical explanation for this difference.

The atmospheric significance of reaction 1f clearly depends on the rate coefficients and also concentrations of gas species

and salt particles. In this article we have measured rate coefficients for (1f) at ambient temperature. However, the concentrations of HNO_3, HBr, NaBr(s), and $NaNO_3$(s) vary drastically in the atmosphere. We will discuss this matter separately for two regions of the atmosphere.

Troposphere. In the marine boundary layer the gas-phase nitric acid mixing ratio is about 1 ppbv.[18,19] It is interesting to investigate the uptake of nitric acid by sea-salt particles. Because concentrations of bromides are about 2 orders of magnitude smaller than chlorides in sea-salt particles[7−9] and the uptake coefficient for (1f) is about a factor of 5 smaller than the uptake of HNO_3 by NaCl, we conclude that HNO_3 predominantly reacts with NaCl rather than NaBr in the marine boundary layer.

In the arctic troposphere there is a strong correlation between ozone loss and filtered bromine (i.e., bromine compounds that can be collected on cellulose filters or Teflon/nylon filters). It is possible that NaBr may be present, in addition to HBr or BrO, in the measurement of filtered bromine. Hence, it is likely that reaction 1f may play a role in the Arctic ozone loss.

Stratosphere. As discussed in the Introduction, chloride particles were observed in the lower stratosphere a few months after the eruption of El Chichon by Woods et al.[14] and a significant enhancement of hydrogen chloride was measured using infrared spectrometry.[15] In our previous articles[10,11] we have suggested that heterogeneous reactions on NaCl particles may be responsible for this enhancement. However, it is possible that small amounts of bromides may accompany the chlorides in volcanic emissions. If NaBr were also injected from El Chichon, reaction 1 could transform the solid bromide salts into hydrogen bromide. To our knowledge, there was no such measurement of the HBr column density made in 1982. The observation would be very difficult because the background concentration is as low as 1−2 pptv.[30] Therefore, it is not possible to conclude that reaction 1f played any role in stratospheric chemistry after the eruption of El Chichon.

Conclusions

In this paper we have reported the kinetic measurements for the forward and reverse processes of reaction 1. The uptake coefficients for $\gamma(1f) = (2.8 \pm 0.5) \times 10^{-3}$ and $\gamma(1r) = (1.2 \pm 0.2) \times 10^{-2}$ were obtained at 296 K, respectively. These uptake processes were found to comprise both physical adsorption and heterogeneous reaction.

Acknowledgment. The research described in this article was performed at the Jet Propulsion Laboratory, California Institute of Technology, under contract with the National Aeronautics and Space Administration. R.S.T. gratefully acknowledges the financial support from the Maj and Tor Nessling Foundation.

References and Notes

(1) Finlayson-Pitts, B. J.; Livingston, F. E.; Berko, H. N. *Nature* **1990**, *343*, 622.
(2) Berko, H. N.; McCaslin, P. C.; Finlayson-Pitts, B. J. *J. Phys. Chem.* **1991**, *95*, 6951.
(3) Fan, S.-M.; Jacob, D. J. *Nature* **1992**, *359*, 522.
(4) Bottenheim, J. W.; et al. *J. Geophys. Res.* **1990**, *95*, 18555.
(5) Oltmans, S. J.; et al. *Atmos. Environ.* **1989**, *23*, 2431.
(6) McConnell, J. C.; et al. *Nature* **1992**, *355*, 150.
(7) Moyers, J. L.; Duce, R. A. *J. Geophys. Res*. **1972**, *77*, 5330.
(8) Duce, R. A.; Zoller, W. H.; Moyers, J. L. *J. Geophys. Res*. **1973**, *78*, 7802.
(9) Sturges, W. T.; Barrie, L. A. *Atmos. Environ*. **1988**, *22*, 1179.
(10) Timonen, R. S.; Chu, L. T.; Leu, M.-T.; Keyser, L. F. *J. Phys. Chem.* **1994**, *98*, 9509.
(11) Leu, M.-T.; Timonen, R. S.; Keyser, L. F.; Yung, Y. L. *J. Phys. Chem.* **1995**, *99*, 13203.
(12) Fenter, F. F.; Caloz, F.; Rossi, M. J. *J. Phys. Chem.* **1994**, *98*, 9801.
(13) Laux, J. M.; Hemminger, J. C.; Finlayson-Pitts, B. J. *Geophys. Res. Lett.* **1994**, *21*, 162
(14) Woods, D. C.; Chuan, R. L.; Rose, W. I. *Science* **1985**, *230*, 170.
(15) Mankin, W. G.; Coffey, M. T. *Science* **1984**, *226*, 170.
(16) Michelangeli, D. G.; Allen, M.; Yung, Y. L. *Geophys. Res. Lett.* **1991**, *18*, 673.
(17) Michelangeli, D. G.; Allen. M.; Yung, Y. L. *J. Geophys. Res.* **1989**, *94*, 18429.
(18) Solomon, P. A.; Salmon, L. G.; Fall, T.; Cass, G. R. *Environ. Sci. Technol.* **1992**, *26*, 1594.
(19) Eldering, A.; Solomon, P. A.; Salmon, L. G.; Fall, T.; Cass, G. R. *Atmos. Environ.* **1991**, *25*, 2091.
(20) Pszenny, A. A. P.; et al. *Geophys. Res. Lett.* **1993**, *20*, 699.
(21) Chu, L. T.; Leu, M.-T.; Keyser, L. F. *J. Phys. Chem.* **1993**, *97*, 7779.
(22) Gregg, S. J.; Sing, K. S. W. *Adsorption, Surface Area and Porosity*, Academic Press: New York, 1982.
(23) Weast, R. C. *Handbook of Chemistry and Physics*, 65th ed.; CRC Press: Boca Raton, FL, 1984.
(24) Kaufman, F. *Prog. React. Kinet.* **1961**, *1*, 1.
(25) Marreo, T. R.; Mason, E. A. *J. Phys. Chem. Ref. Data* **1972**, *1*, 3.
(26) Keyser, L. F.; Moore, S. B.; Leu, M.-T. *J. Phys. Chem.* **1991**, *95*, 5496.
(27) Keyser, L. F.; Leu, M.-T.; Moore, S. B. *J. Phys. Chem.* **1993**, *97*, 2800.
(28) Satterfield, C. N. *Heterogeneous Catalysis in Industrial Practice*, 2nd ed.; McGraw-Hill: New York, 1991.
(29) Fenter, F. F.; Caloz, F.; Rossi, M. J. *J. Phys. Chem.* **1996**, *100*, 1008.
(30) Johnson, D. G.; Traub, W. A.; Chance, K. V.; Jucks, K. W. *Geophys. Res. Lett.* **1995**, *22*, 1373.